Available online at www.sciencedirect.com
SCIENCE DIRECT®

Journal of the European Ceramic Society 24 (2004) 1271–1275
www.elsevier.com/locate/jeurceramsoc

Transport properties of $La_{0.6}Y_{0.1}Ca_{0.3}MnO_3$ compounds with different interfaces

F.C. Fonseca[a,e], J.A. Souza[a], R.F. Jardim[a,*], R. Muccillo[b], E.N.S. Muccillo[b], D. Gouvêa[c], M.H. Jung[d], A.H. Lacerda[d]

[a]*Instituto de Física, Universidade de São Paulo, São Paulo, SP, Brazil*
[b]*CMDMC, CCTM-Instituto de Pesquisas Energéticas e Nucleares, São Paulo, SP, Brazil*
[c]*Departamento de Engenharia Metalúrgica e de Materiais, Escola Politécnica, USP, São Paulo, SP, Brazil*
[d]*National High Magnetic Field Laboratory, Los Alamos National Laboratory, Los Alamos, NM, USA*
[e]*CCTM-Instituto de Pesquisas Energéticas e Nucleares, São Paulo, SP, Brazil*

Abstract

The electrical resistivity $\rho(T)$, magnetoresistivity $\rho(T,H)$, and impedance spectroscopy $Z(\omega,T)$ of polycrystalline $La_{0.6}Y_{0.1}Ca_{0.3}MnO_3$ compounds with different intergranular surfaces were investigated. The interfaces were modified through controlled addition of pores in samples prepared by the sol-gel technique. X-ray diffraction, scanning electron microscopy, and mercury porosimetry analysis showed that all specimens are single phase having similar microstructures and differing only by the volume fraction of pore. $\rho(T,H)$ and $Z(\omega,T)$ data revealed that all samples undergo a metal-insulator transition at $T\sim175$ K. In addition, the $Z(\omega,T)$ data indicate two well defined contributions to the electrical resistivity. The $\rho(T,H)$ data exhibit features of colossal magnetoresistivity CMR phenomenon but were found to be independent of porosity. The combined results suggest that the CMR effect is mainly associated with percolation of metallic regions and weakly dependent on sample morphology.

Keywords: Perovskites; Porosity; Magnetoresistance; Impedance

1. Introduction

Mixed-valence manganites $(R_{1-x}A_x)MnO_3$ (R = rare-earth, A = alkali or alkaline earth) with perovskite structure exhibit a rich variety of physical properties. Specifically, $La_{1-x}Ca_xMnO_3$ compounds have been extensively studied and their corresponding magnetic phase diagram was previously reported.[1] In the x range from 0.2 to 0.5 these compounds exhibit ferromagnetism and metallic conductivity owing to the interaction between Mn^{3+}–Mn^{4+} pairs. The Mn^{4+} ions are created by the partial substitution of a divalent alkaline earth for trivalent lanthanum. In particular, the influence of La^{3+} substitution for Y^{3+} on $La_{1-x}Ca_xMnO_3$ has already been reported.[2,3] The main effect of such a substitution is the modification of the Mn–O–Mn bond angle due to smaller ionic radius of Y^{3+}. The distortion of this bond angle changes carrier mobility, increasing the electrical resistivity without changing carrier concentration.

As far as the origin of the CMR effect is concerned, two mechanisms are of special interest. The first is the phase separation PS which suggests that the arrangement of the Mn^{3+}–Mn^{4+} pairs are confined to submicrometric regions in these materials. Both spectroscopic[4] and macroscopic[5,6] measurements along with theoretical works have provided evidence for the PS in these manganites. The experimental measurements indicated that in $La_{1-x}Ca_xMnO_3$-type compounds (with $x=0.3$) two spatially separated phases coexist: a ferromagnetic metallic FMM phase and a paramagnetic/antiferromagnetic insulating P/AFMI phase.[4] The relative volume fraction of these phases is determined by varying temperature and/or magnetic field, leading to a percolative metal-insulator MI transition at temperatures T_{CR}. The latter is close to the Curie temperature of the system.

The second mechanism is related to the intergranular influence on the transport properties of manganites,

* Corresponding author. Tel.: +55-11-818-6896; fax: +55-11-818-6984.
E-mail address: rjardim@if.usp.br (R.F. Jardim).

0955-2219/03/$ - see front matter © 2003 Elsevier Ltd. All rights reserved.
doi:10.1016/S0955-2219(03)00446-1

known as intergranular magnetoresistivity IMR.[8,9] Such an effect is defined as a large drop of the electrical resistance of these ceramics at relatively low applied magnetic fields. Magnetoresistivity measurements in manganites revealed that polycrystalline samples exhibit a large IMR effect while such an effect was found to be nearly absent in single crystals.[8] Thus, the IMR effect was attributed to a spin-polarized tunneling between ferromagnetic grains of these materials.[8] Following this work, several studies concerning the dependence of the CMR effect on the grain boundary density of manganites have been reported.[8,9] Actually, these studies are based on the modification of the intergranular surfaces by changing the average grain size of the ceramics through heat treatments.[9] Such a procedure usually results in specimens with different internal surface densities but also with different MI transition temperatures T_{CR}.

Based on the above discussion, our focus in the present work is to obtain polycrystalline samples of $La_{0.6}Y_{0.1}Ca_{0.3}MnO_3$ with similar T_{CR} but with different intergranular surfaces in order to further investigate the transport properties of these manganites.

2. Experimental

Single phase $La_{0.6}Y_{0.1}Ca_{0.3}MnO_3$ ceramics were prepared through sol-gel precursors and details of the sample preparation are described elsewhere.[10] To investigate the role played by intergranular properties on the transport mechanisms, the internal surfaces of polycrystalline samples were modified by the controlled introduction of porosity P. This was done through the addition of spherical polymeric particles of low-density polyethylene (Aldrich). These particles were mixed to the manganite powders in proportions of 0, 10, 20, and 30 vol.% (hereafter referred as P0, P10, P20, and P30 samples, respectively) and pressed into pellets. Sintering, and consequent polymer elimination, was performed in a single heat treatment at 900 °C for 30 h in air.

Ground samples were analyzed by X-ray powder diffraction XRD at room temperature in the $20^\circ \leqslant 2\theta \leqslant 80^\circ$ range. Fractured surfaces were observed in a scanning electron microscope SEM for microstructural characterization. Pore distribution was determined by mercury porosimetry MP.

Four-wire magnetoresistivity $\rho(T,H)$ measurements were performed in the temperature range $2 \leqslant T \leqslant 300$ K and applied magnetic fields to 18 T. Two-probe impedance spectroscopy $Z(\omega,T)$ measurements were carried out from 77 to 300 K in the 5 Hz–13 MHz frequency range. In all transport measurements, copper electrical leads attached to Ag film contact pads on parallelepiped-shaped samples were used.

3. Results and discussion

The XRD analysis (not shown) of the P0 and P30 samples revealed that all the observed peaks belong to the $La_{0.6}Y_{0.1}Ca_{0.3}MnO_3$ phase, space group *Pnma* (N. 62). The calculated lattice parameters were found to be in excellent agreement with previously reported data.[11] In addition, the XRD patterns revealed the absence of extra reflections belonging to any additional phase in samples with polymer addition. These results suggest that the polymeric particles were completely removed during the heat treatment and that neither polymeric residues nor chemical reaction between the ceramic phase and the polymer were detected within the resolution of the XRD technique.

The MP measurements (not shown) revealed a narrow pore size distribution, ranging from 0.1 to 0.6 μm in the P0 sample. All the other samples were found to have wider pore distributions, typically between 0.1 and 70 μm, and the pore volume fraction was found to increase with increasing nominal content of polymer. The average pore size was found to be approximately 0.22 μm for all samples studied. The features observed in the MP measurements were mirrored in the SEM micrographs, as displayed in Fig. 1. The SEM images indicate that the P0 sample has a more agglomerated microstructure in comparison with the sample with higher P. In fact, the P30 specimen resembles a more granular microstructure with larger intergrain separations than P0. Indeed, an accurate analysis of the derivative of the MP curves allowed us to conclude that the P30 specimen has 30%

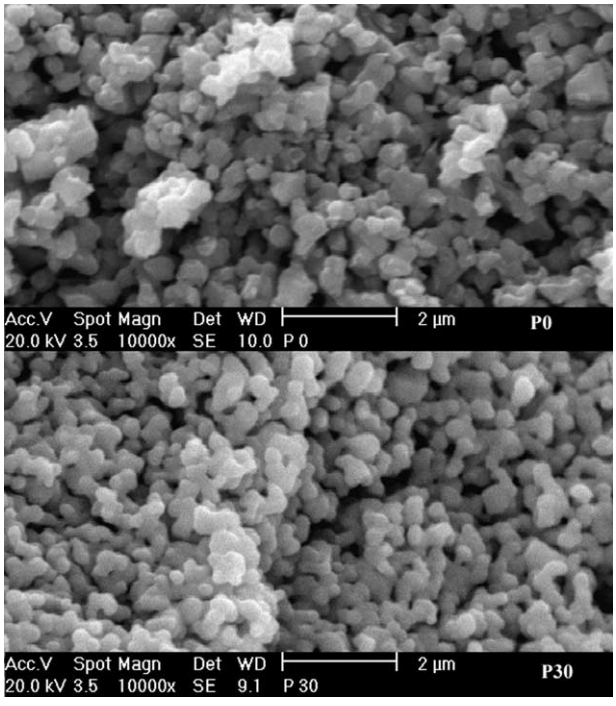

Fig. 1. Scanning electron micrographs of $La_{0.6}Y_{0.1}Ca_{0.3}MnO_3$ samples with low porosity (P0) and 30 vol.% porosity (P30).

higher volume fraction of pores than the P0 specimen in the region of 0.09–0.5 μm, which is the appropriated size scale to study intergranular effects in these specimens. The SEM analysis also indicates that increasing P has minor effect on both grain shape and average size, which was found to be 0.5 μm for P0 and P30 samples.

Once we have obtained single phase ceramics with similar microstructures differing only by the volume fraction of pores, let us concentrate on the transport properties of the samples. The temperature dependence of the electrical resistivity $\rho(T)$ (Fig. 2) showed that all curves have similar behavior and exhibit a typical MI transition at the same temperature $T_{CR} \sim 175$ K. The $\rho(T)$ data also reveal that increasing P results in larger magnitudes of $\rho(T)$ and that such a feature is much more pronounced at temperatures close to T_{CR}. This increase of $\rho(T)$ is certainly related to the scattering of charge carriers due to increasing density of interfaces. In fact, the $\rho(T)$ behavior at temperatures $T > T_{CR}$ was found to follow an Arrhenius-type activated process. An analysis of the temperature-independent electrical resistivity ρ_0 and the activation energy ΔE obtained after fittings indicate that all samples have approximately the same activation energy ($\sim$140 meV) and that ρ_0 increases with increasing P. The studied specimens have the same density of charge carriers, thus the already expected increase of ρ_0 with increasing P could be related to the decrease of the mobility of charge carriers due to the increasing scattering by pores.

In order to study the influence of internal surfaces and the PS in these manganites, IS measurements have been performed (Fig. 3). The $Z(\omega,T)$ data show two well defined semicircles in the whole frequency and temperature ranges studied: one occurring at high frequencies, which is denoted by HF, and another one, at low frequencies, referred to as LF.[10] This indicates that

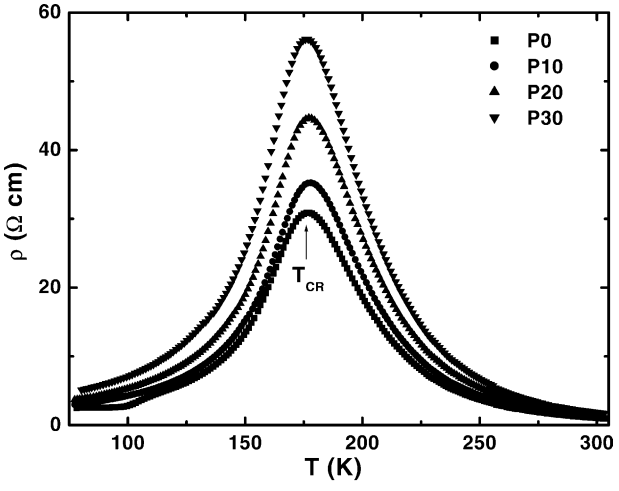

Fig. 2. Temperature dependence of the electrical resistivity of $La_{0.6}Y_{0.1}Ca_{0.3}MnO_3$ samples with 0, 10, 20, and 30 vol.% of porosity.

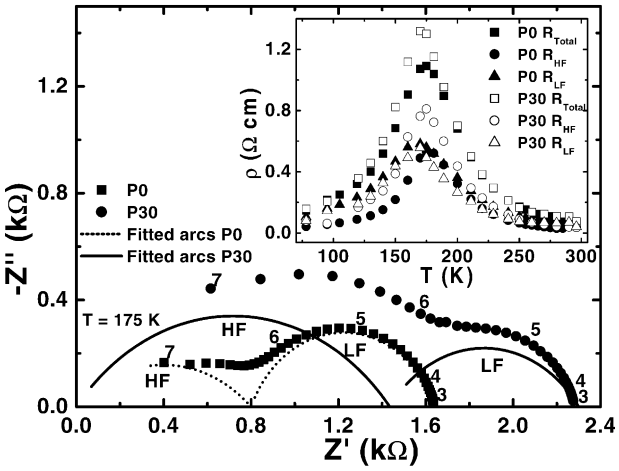

Fig. 3. Impedance diagrams of $La_{0.6}Y_{0.1}Ca_{0.3}MnO_3$ sampies with 0 (full squares) and 30 vol.% (full circles) of pore measured at 175 K. Fitted semicircles are also shown in solid and dashed lines. Numbers indicate the logarithm of the signal frequency. The inset shows the temperature dependence of the electrical resistivity determined from the $Z(\omega,T)$ data: R_{HF} corresponds to the electrical resistivity associated to the high frequency semicircle, R_{LF} to the low frequency one, and R_{Total} is defined as $R_{HF} + R_{LP}$.

at least two different transport processes occur in the frequency range studied.

Fitting the measured IS diagrams at different temperatures allowed us to separate the two contributions to the electrical resistivity, which are referred as R_{HF} and R_{LF}, as shown on the inset of Fig. 3. Both components exhibit a MI transition occurring at 175 K, in excellent agreement with $\rho(T)$ data. Furthermore, samples with different interface density have comparable R_{LF} amplitudes but differ on R_{HF} amplitudes.

Assuming an activation process for $T > T_{CR}$, the thermal activation energy ΔE for both HF and LF processes were determined for the P0 and P30 samples. The obtained ΔE values for both R_{HF} ($\sim$135 meV) and $\rho_{dc}(T)$ ($\sim$140 meV) are comparable and the R_{LF} has smaller ΔE values ($\sim$105 meV). The ΔE values for the R_{LF} component are in good agreement with previously reported values ($\sim$100 meV) obtained from $\rho_{dc}(T)$ measurements for the parent compound.[12] The results of the thermal activation energy for electrical conduction suggest that the transport mechanism of HF and LF components are not equivalent. Moreover, they indicate that the LF component is not related to a grain boundary relaxation process, since a relaxation due to interfacial scattering of charge carriers would have a $\sim$20% larger ΔE value than a bulk one.[13] Therefore, our experimental results do not seem to follow the predictions of a bulk-grain boundary picture: the LF resistivity R_{LF} decreases with decreasing T below T_{CR} and has a lower ΔE value in the thermally activated regime. In fact, due to the electronic nature of charge carriers in manganites and its relatively high electrical conductivity, this material is not supposed to exhibit a

relaxation on the IS diagram due to a blocking process through grain boundaries. Such a behavior is usually observed for low electrical conductivity materials with ionic charge carriers.[13] These observations constitute further evidence of a relaxation process due to a different phase.

Thus, the HF and LF components may be related to different phases within physical grains or even clusters. Such a coexistence of different phases or clusters is expected in a PS scenario where the presence of distinct magnetic micro domains are frequently observed.[5–7] The IS data confirm the already reported behavior of the two components (HF and LF) which were attributed to different clusters of magnetic phases.[10] These results are also in excellent agreement with recent results of Mössbauer spectroscopy experiments on the same material. They suggested a coexistence FMM and P/AFMI phases, in temperatures close to T_{CR}, which compete with each other in a percolative process.[14]

Based on the above results, it is possible to visualize these ceramics as comprised of grains in which at least two microscopic phases or clusters coexist and have a percolative transition at T_{CR}.[10] Thus, to further investigate the effect of increasing P on the electrical behavior of our samples, magnetoresistivity measurements ρ(H,T) were performed, as shown in Fig. 4. We have observed that the $\rho(H)/\rho(H=0)$ ratio decreases appreciably ($\sim$50%) up to 3 T for both samples, which characterizes the negative IMR effect.[8] Increasing H results in a much less pronounced decrease of $\rho(H)/\rho(H=0)$ and for $H>5$ T the magnetoresistivity have a weak dependence on the applied magnetic field.[8] This general behavior of $\rho(H)/\rho(H=0)$ versus H occurs for temperatures varying from 2 K to just above T_{CR} and the largest drop ($\sim$95%) is observed at $T\sim T_{CR}$. However, the most important feature to point out is that the $\rho(H,T)$ data taken on specimens with modified intergrain surfaces

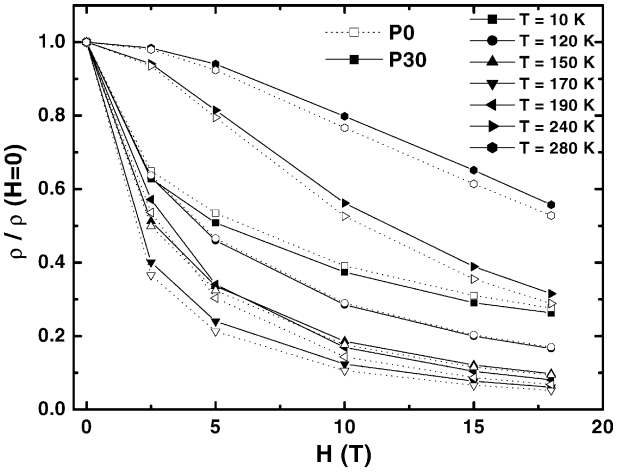

Fig. 4. Values of the normalized magnetoresistivity $\rho(H)/\rho(H=0)$ as a function of the applied magnetic field for $La_{0.6}Y_{0.1}Ca_{0.3}MnO_3$ samples with 0 (open symbols) and 30 vol.% (full symbols) porosity.

suggest that the CMR effect is weakly dependent on the intergranular surface. In fact, the $\rho(H)/\rho(H=0)$ curves taken on both samples have essentially the same behavior in the whole temperature range investigated. Furthermore, the $\rho(T,H)$ data presented here indicate that the CMR effect is independent on intergrain surfaces. Thus, the combined experimental results indicates that spin-polarized tunneling may also occur between conducting FMM clusters through P/AFMI clusters and not necessarily only across grain boundaries.[15]

4. Conclusion

In summary, we have successfully modified the internal surfaces of polycrystalline $La_{0.6}Y_{0.1}Ca_{0.3}MnO_3$ samples through the addition of a polymer with no apparent changes on grain morphology and chemical composition. Specimens with different porosity exhibited nearly the same metal-insulator transition temperature and thermal activation energy for electrical conduction. Impedance spectroscopy measurements revealed two well defined contributions to the electrical transport. These components were related to two phases within physical grains or clusters with different transport properties. Magnetoresistivity measurements on samples with different porosity show no appreciable changes, indicating that the spin-polarized tunneling may not occur necessarily across intergrain surfaces. Tunneling of carriers between conducting ferromagnetic domains or clusters separated by semiconducting paramagnetic/antiferromagnetic interfaces is more likely to occur in these manganites.

Acknowledgements

This work was supported by FAPESP under Grant Nos. 99/10798-0, 01/04231-0, and 99/11654-2. R.F.J. and E.N.S.M. are CNPq fellows under Grants Nos. 304647/90-0 and 300934/94-7, respectively. The support of NSF Grant. No. INT-9725929 (A.H.L.) and CNPq (R.F.J.) are gratefully acknowledged. Work at the NHMFL was performed under the auspices of the NSF, the state of Florida, and the USDOE.

References

1. Schiffer, P., Ramirez, A. P., Bao, W. and Cheong, S. W., Low-temperature magnetoresistance and the magnetic phase-diagram of $La_{1-x}Ca_xMnO_3$. *Phys. Rev. Lett.*, 1995, **75**, 3336–3339.
2. Fontcuberta, J., Martínez, B., Seffar, A., Piñol, S., Garcia-Muñoz, J. L. and Obradors, X., Colossal magnetoresistance of ferromagnetic manganites: structural tuning and mechanisms. *Phys. Rev. Lett.*, 1996, **76**, 1122–1125.
3. Hwang, H. Y., Cheong, S.-W., Radaelli, P. G., Marezio, M. and

Batlogg, B., Lattice effects of the magnetoresistance in doped $LaMnO_3$. *Phys. Rev. Lett.*, 1995, **75**, 914–917.
4. Kapusta, Cz., Riedi, P. C., Sikora, M. and Ibarra, M. R., NMR probe of phase segregation in electron doped mixed valence manganites. *Phys. Rev. Lett.*, 2000, **84**, 4216–4219.
5. Fäth, M., Freisem, S., Menovsky, A. A., Tomioka, Y., Aarts, J. and Mydosh, J. A., Spatially inhomogeneous metal-insulator transition in doped manganites. *Science*, 1999, **285**, 1540–1542.
6. Uehara, M., Mori, S., Chen, C. H. and Cheong, S. W., Percolative phase separation underlies colossal magnetoresistance in mixed-valent manganites. *Nature*, 1999, **399**, 560–563.
7. Moreo, A., Yunoki, S. and Dagotto, E., Phase separation scenario for manganese oxides and related materials. *Science*, 1999, **283**, 2034–2040.
8. Hwang, H. Y., Cheong, S.-W., Ong, N. P. and Batlogg, B., Spin-polarized intergrain tunneling in $La_{2/3}Sr_{1/3}MnO_3$. *Phys. Rev. Lett.*, 1996, **77**, 2041–2044.
9. Fu, Y. L., Grain-boundary effects on the electrical resistivity and the ferromagnetic transition temperature of $La_{0.8}Ca_{0.2}MnO_3$. *Appl. Phys. Lett.*, 2000, **77**, 118–120.
10. Souza, J. A., Jardim, R. F., Muccillo, R., Muccillo, E. N. S., Torikachvili, M. S. and Neumeier, J. J., Impedance spectroscopy evidence of the phase separation in $La_{0.3}Pr_{0.4}Ca_{0.3}MnO_3$ manganite. *J. Appl. Phys.*, 2001, **89**, 6636–6638.
11. Wang, Y. X., Du, Y., Qin, R. W., Han, B., Du, J. and Lin, J. H., Phase equilibrium of the La–Ca–Mn–O system. *J. Solid State Chem.*, 2001, **156**, 237–241.
12. Zhou, S. M., Zhou, G. E. and Zhang, Y. H., Effects of lattice distortion on the electrical transport in Ca-deficient $La_{0.67}Ca_{0.33-x}MnO_{3-\delta}$ ($0 \leqslant x \leqslant 0.15$) polycrystals. *Physica B*, 2000, **279**, 257–261.
13. Kleitz, M., Dessemond, L. and Steil, M. C., Model for ion-blocking at internal interfaces in zirconias. *Solid State Ionics*, 1995, **75**, 107–115.
14. Goya, G. F., Souza, J. A. and Jardim, R. F., Mössbauer spectroscopy and magnetoresistivity of Fe-57 substituted Mn in $La_{0.7-x}Y_xCa_{0.3}MnO_3$ manganites. *J. Appl. Phys.*, 2002, **91**, 7932–7934.
15. Fonseca, F. C., Souza, J. A., Jardim, R. F., Muccillo, R., Mucillo, E. N. S., Gouvêa, D., Jung, M. H., and Lacerda, A. H., Transport properties and phase separation in $La_{0.6}Y_{0.1}Ca_{0.3}MnO_3$ ceramics. *Phys. Stat. Sol.*, 2003, accepted.